

¹ **A regional peaks-over-threshold model in a nonstationary** ² **climate**

M. Roth^{1,2}, T. A. Buishand², G. Jongbloed³, A. M. G. Klein Tank², and J. H.

van Zanten¹

M. Roth and J. H. van Zanten, EURANDOM, Eindhoven University of Technology, PO Box 513, Eindhoven, 5600 MB, Netherlands. (m.roth@tue.nl; J.H.v.Zanten@tue.nl)

T. A. Buishand and A. M. G. Klein Tank, Royal Netherlands Meteorological Institute, PO Box 201, 3730 AE De Bilt, Netherlands. (buishand@knmi.nl; albert.klein.tank@knmi.nl)

G. Jongbloed, Delft Institute of Applied Mathematics, Delft University of Technology, Mekelweg 4, 2628 CD Delft, Netherlands. (G.Jongbloed@tudelft.nl)

¹EURANDOM, Eindhoven University of
Technology, Netherlands

²Royal Netherlands Meteorological
Institute, De Bilt, Netherlands.

³Delft Institute of Applied Mathematics,
Delft University of Technology,
Netherlands

3 **Abstract.** Regional frequency analysis (RFA) is often used to reduce
4 the uncertainty in the estimation of distribution parameters and quan-
5 tiles. In this paper a regional peaks-over-threshold (POT) model is intro-
6 duced that can be used to analyze precipitation extremes in a changing
7 climate. We use a temporally varying threshold, which is determined by
8 quantile regression for each site separately. The marginal distributions
9 of the excesses are described by generalized Pareto (GP) distributions.
10 The parameters of these distributions may vary over time and their spa-
11 tial variation is modeled by the index flood (IF) approach. We consider
12 different models for the temporal dependence of the GP parameters. Pa-
13 rameter estimation is based on the framework of composite likelihood.
14 Composite likelihood ratio tests that account for spatial dependence are
15 used to test the significance of temporal trends in the model parameters
16 and to test the IF assumption.
17 We apply the method to gridded, observed daily precipitation data from
18 the Netherlands for the winter season. A general increase of the thresh-
19 old is observed, especially along the west coast and northern parts of the
20 country. This implies, that moderate extremes have increased over the
21 observed time period. Moreover, the positive trend in the threshold in-
22 duces an increase in the scale parameter of the GP distribution owing to
23 the IF assumption. There is no additional trend in the scale parameter
24 and the trend in the shape parameter is not significant.

1. Introduction

25 Design values for infrastructure are often based on characteristics of extreme precipi-
26 tation. These characteristics may have changed over time owing to climate change, see
27 e.g. *Klein Tank and Können* [2003] and *Milly et al.* [2008], which contradicts the station-
28 arity assumption, that is usually made in hydrologic and hydraulic design. Wrongly
29 assuming stationarity generally leads to systematic errors in design values and might
30 have a considerable impact on the risk of failure of hydraulic structures, as shown by
31 *Wigley* [2009]. Climate scientists have analyzed trends in moderate extremes, that oc-
32 cur once or several times per year, based on annual indices. Examples are the empirical
33 annual 90% quantile of the precipitation amounts on wet days or the 1-day or 5-day
34 maximum precipitation amount in each year, see e.g. *Klein Tank and Können* [2003] and
35 *Turco and Llasat* [2011].

36 In this study we focus on rare extremes which occur less frequently than once per
37 year. These are frequently assessed by extreme value (EV) models. To account for the
38 temporal trend in the distribution, the parameters of the EV model are often selected
39 to be time dependent [*Smith*, 1986; *Kharin and Zwiers*, 2005; *Brown et al.*, 2008; *Hanel et*
40 *al.*, 2009; *Kyselý et al.*, 2010; *Beguería et al.*, 2011]. Because of the rarity of the extremes,
41 the parameters in these EV models and, especially, large quantiles of the precipitation
42 amounts have wide confidence intervals. To reduce the uncertainty in the estimates
43 the use of data sets over a long period and/or regional frequency analysis (RFA), have
44 been recommended e.g. by *Hosking and Wallis* [1997]. Data sets over a long period are
45 often only available for a few stations, whereas we have multiple stations that cover a

46 relatively short time period. The idea behind RFA is to exploit the similarities between
47 the sites in a certain region, so that all data in the region can be used to obtain quantile
48 estimates for a particular site. The index flood (IF) approach is a popular method in
49 RFA. It assumes that the distributions of the extreme precipitation amounts are identi-
50 cal after scaling with a site-specific factor (the index flood).

51 The IF approach has frequently been applied to describe the distribution of block
52 maxima (BM), i.e. the largest value in a year or season. Considering only BM discards
53 useful data in the case of multiple extremes in a block, see e.g. *Madsen et al.* [1997a]
54 and *Kyselý et al.* [2010]. An alternative method to analyze extremes is to consider all
55 values that exceed a certain high threshold, which is known as peaks-over-threshold
56 (POT) modeling. A potential advantage of POT modeling is the possibility to include
57 more data in the analysis than in the BM approach, which may reduce the estimation
58 variance. The use of the IF assumption together with the POT approach has been stud-
59 ied in *Madsen and Rosbjerg* [1997] for stationary data. Here we develop a different POT
60 model with time-varying parameters, that satisfies the IF assumption.

61 In section 2 we describe the proposed model. We explain the basic methods used
62 to deal with high quantile estimation in the case of stationary data with emphasis on
63 the POT approach. After that, we present our model for the nonstationary climate. In
64 section 3 we outline the estimation procedure. The choice between different models is
65 addressed in section 4 and in section 5 the application of the model to observed daily
66 precipitation data in the Netherlands is discussed.

2. Model description

67 The data we describe with our model consist of measurements at S sites over a period
68 of T time points. The data can be represented in an $S \times T$ space-time matrix

$$69 \quad \mathbf{X} := (X_s(t))_{s \in \mathcal{S}, t \in \mathcal{T}},$$

70 where $X_s(t)$ is the random variable representing the value at site s and time t , $\mathcal{S} :=$
71 $\{1, \dots, S\}$ and $\mathcal{T} := \{1, \dots, T\}$.

72 In POT modeling exceedances over a high threshold $u_s(t)$ are considered, $s \in \mathcal{S}$,
73 $t \in \mathcal{T}$. This threshold is generally site specific and may depend on time. In the case of
74 temporal clustering of the exceedances the largest value in a cluster (peak) is consid-
75 ered only. These peaks will then generally be approximately independent. We assume
76 that the $X_s(t)$ have been declustered and we define $Y_s(t)$ as the difference between the
77 daily value at site s and time t and the corresponding value of the threshold, i.e.

$$78 \quad Y_s(t) := X_s(t) - u_s(t),$$

79 and \mathbf{Y} is defined analogously to \mathbf{X} . The excesses are the nonnegative part of \mathbf{Y} . Note,
80 that due to the declustering $Y_s(t)$ is only non-negative if there is a peak. By $\tilde{\mathcal{T}}$ we
81 denote the subset of days which exhibit at least one exceedance of the threshold, i.e.

$$82 \quad \tilde{\mathcal{T}} := \{t \in \mathcal{T} \mid \exists s \in \mathcal{S} : Y_s(t) \geq 0\}.$$

2.1. Stationary climate

83 2.1.1. Site specific approach

84 The BM approach for a stationary climate relies on the Fisher-Tippet-Gnedenko the-
85 orem for maxima of independent and identically distributed (i.i.d.) random variables.
86 This theorem allows, under certain regularity conditions, to approximate the distribu-
87 tion of the BM by an extreme value distribution, see e.g. *Embrechts et al.* [1997]. The

three types of extreme value distributions can be summarized in the generalized extreme value (GEV) distribution, i.e.

$$H_{\tilde{\zeta}^*, \sigma^*, \mu^*}(x) = \begin{cases} \exp \left\{ - \left[1 + \tilde{\zeta}^* \left(\frac{x - \mu^*}{\sigma^*} \right) \right]^{-1/\tilde{\zeta}^*} \right\}, & \tilde{\zeta}^* \neq 0, \\ \exp \left[- \exp \left(- \frac{x - \mu^*}{\sigma^*} \right) \right], & \tilde{\zeta}^* = 0, \end{cases}$$

for $1 + \tilde{\zeta}^*(x - \mu^*)/\sigma^* > 0$, where μ^* , σ^* and $\tilde{\zeta}^*$ are the location, scale and shape parameter. $\tilde{\zeta}^* > 0$ corresponds to the Fréchet family, $\tilde{\zeta}^* < 0$ to the Weibull family and $\tilde{\zeta}^* = 0$ to the Gumbel family.

When we consider the POT approach rather than block maxima, we have to model the process of exceedance times and the distribution of the excesses separately. In a stationary climate the threshold u is constant and the times of exceedance are usually modeled by a homogeneous Poisson process. This implies, that the mean number λ of exceedances in a block (i.e., year or a particular season) is constant over time.

The Balkema-de Haan-Pickands theorem states, that the distribution of i.i.d. excesses can be approximated by a generalized Pareto (GP) distribution, if the threshold u is sufficiently high and certain regularity conditions hold, see e.g. *Reiss and Thomas [2007]*:

$$P(Y \leq y | Y \geq 0) = G_{\tilde{\zeta}, \sigma}(y) = \begin{cases} 1 - \left(1 + \frac{\tilde{\zeta}y}{\sigma} \right)^{-1/\tilde{\zeta}}, & \tilde{\zeta} \neq 0, \\ 1 - \exp \left(- \frac{y}{\sigma} \right), & \tilde{\zeta} = 0, \end{cases}$$

for $y \geq 0$ if $\tilde{\zeta} \geq 0$ and $0 \leq y \leq -\sigma/\tilde{\zeta}$ if $\tilde{\zeta} < 0$, where σ and $\tilde{\zeta}$ are the scale and the shape parameter. For $\tilde{\zeta} = 0$ the GP distribution reduces to the exponential distribution.

We are interested in the level q_α which is exceeded on average α times in a block. Since there are on average λ peaks in a block, the probability that an arbitrary peak exceeds this level equals α/λ . To obtain q_α we first determine the $(1 - \alpha/\lambda)$ -quantile

110 of the excess distribution:

$$111 \quad \tilde{q}_\alpha = G_{\tilde{\xi}, \sigma}^{-1}(1 - \alpha/\lambda),$$

112 and then add the threshold u , i.e.

$$113 \quad q_\alpha = u + \tilde{q}_\alpha = \begin{cases} u + \frac{\sigma}{\tilde{\xi}}[1 - (\frac{\alpha}{\lambda})^{-\tilde{\xi}}], & \tilde{\xi} \neq 0, \\ u + \sigma \ln(\frac{\lambda}{\alpha}), & \tilde{\xi} = 0. \end{cases} \quad (1)$$

114 We will sometimes indicate the quantile q_α as the $1/\alpha$ return level to make the com-
115 parison with studies for a stationary climate easier.

116 If one assumes that the exceedance times originate from a homogeneous Poisson pro-
117 cess and the excesses are independent and follow a GP distribution, it can be shown
118 that the subsequent relationship between the parameters of the GEV and the GP distri-
119 bution holds [Buishand, 1989; Wang, 1991; Madsen et al., 1997b]:

$$120 \quad \begin{aligned} \mu^* &= \begin{cases} u - \frac{\sigma}{\tilde{\xi}}(1 - \lambda^{\tilde{\xi}}), & \tilde{\xi} \neq 0, \\ u + \sigma \ln(\lambda), & \tilde{\xi} = 0, \end{cases} \\ \sigma^* &= \sigma \lambda^{\tilde{\xi}} \\ \tilde{\xi}^* &= \tilde{\xi} \end{aligned} \quad (2)$$

121 Note, that the derived GEV distribution is defined only for BM greater than u .

122 2.1.2. Regional approach

123 The IF method was originally developed for annual maxima of river discharges by
124 Dalrymple [1960]. It assumes that the annual maxima at different sites, after being
125 scaled by a site specific factor, the 'index flood', have a common distribution [e.g. Dal-
126 rymple, 1960; Hosking and Wallis, 1997; Robinson and Sivapalan, 1997]:

$$127 \quad P\left(\frac{M_s}{\eta_s} \leq x\right) = \phi(x) \quad \forall s \in \mathcal{S} \quad (3)$$

128 where M_s represents a typical block maximum at site s , η_s is the index flood at site
129 s for $s \in \mathcal{S}$ and the common distribution function ϕ does not depend on the site s .

130 From equation (3) we see, that the site specific quantile function can be written in the
 131 following product form:

$$132 \quad q_\alpha(s) := Q_{M_s}(\alpha) = \eta_s \phi^{-1}(\tau), \quad (4)$$

133 where Q_{M_s} is the quantile function of M_s and τ is the non-exceedance probability.

134 Because of using more data than those from the site of interest alone, the IF can
 135 provide quantile estimates, which are superior to at-site estimates, even if spatial ho-
 136 mogeneity is not entirely achieved after scaling [Cunnane, 1988]. The IF approach was
 137 developed for river discharges but can be applied, whenever multiple samples of simi-
 138 lar data are available, see *Hosking and Wallis* [1997]. In particular, for precipitation data
 139 the IF assumption has often been used combined with the GEV family, see e.g. *Hosking*
 140 *and Wallis* [1997]; *Fowler et al.* [2005] and *Hanel et al.* [2009]. To further enhance the us-
 141 age of the available data, *Madsen and Rosbjerg* [1997] propose the combination of the IF
 142 assumption with the POT approach.

143 A natural analogue of relation (3) in the POT setting is that the site-specific ex-
 144 ceedances, properly scaled by their index floods, have a common distribution. More
 145 formally:

$$146 \quad P\left(\frac{X_s}{\eta_s} \leq x | X_s \geq u_s\right) = \psi(x) \quad \forall s \in \mathcal{S}, \quad (5)$$

147 where X_s represents the values at site s , η_s is the site-dependent scaling factor (index
 148 flood) and ψ does not depend on site s . Note that because of $\psi(u_s/\eta_s) = 0, \forall s \in \mathcal{S}$ and
 149 because ψ has a density with mass immediately to the right of u_s/η_s , it follows that
 150 u_s/η_s has to be the lower endpoint of the support of ψ for every $s \in \mathcal{S}$, i.e.

$$151 \quad \frac{u_i}{\eta_i} = \frac{u_j}{\eta_j} \quad \forall i, j \in \mathcal{S}. \quad (6)$$

152 This can be only true, if the index flood is a multiple of the threshold, i.e.

$$153 \quad \eta_s = cu_s \quad \forall s \in \mathcal{S},$$

154 for some positive constant c . Without loss of generality we can take $c = 1$. This choice
155 of η_s also satisfies the IF equation for the excesses, i.e.

$$156 \quad P\left(\frac{Y_s}{\eta_s} \leq y | Y_s \geq 0\right) = \tilde{\psi}(y) \quad \forall s \in \mathcal{S}, \quad (7)$$

157 where $\tilde{\psi}(y) := \psi(y + 1)$ is independent of site s .

158 A natural choice for a site specific threshold is a high empirical quantile of the at-site
159 data [see also *Smith, 1989a*]. An important consequence of this choice is that the mean
160 number of exceedances per block λ_s will be approximately constant over the region,
161 i.e.

$$162 \quad \lambda_s \equiv \lambda.$$

163 Under the previous assumptions the distribution of the scaled excesses has the fol-
164 lowing form:

$$165 \quad P\left(\frac{Y_s}{u_s} \leq y | Y_s \geq 0\right) = G_{\xi_s, \frac{\sigma_s}{u_s}}(y). \quad (8)$$

166 Equation (7) then implies, that we have the following restrictions on the parameters of
167 the GP distribution

$$168 \quad \frac{\sigma_s}{u_s} \equiv \gamma, \quad \xi_s \equiv \xi \quad \forall s \in \mathcal{S}, \quad (9)$$

169 for a common dispersion coefficient γ and a common shape parameter ξ .

170 We would like to obtain an IF model in the BM setting, if we transfer the parame-
171 ters from the IF model in the POT setting, using relationship (2). If the block maxima
172 follow a GEV distribution, it can be shown that the IF assumption is satisfied if the

173 dispersion coefficient $\gamma_s^* := \sigma_s^* / \mu_s^*$ and the shape parameter ξ_s^* of the GEV distribution
 174 are constant over the region, see e.g. *Hanel et al.* [2009], i.e.

$$175 \quad \gamma_s^* \equiv \gamma^*, \quad \xi_s^* \equiv \xi^*, \quad \forall s \in \mathcal{S}. \quad (10)$$

176 If we transform the conditions (9) according to relationship (2) and use that λ is con-
 177 stant over the region, we obtain the following conditions on the GEV distribution pa-
 178 rameters:

$$179 \quad \xi_s^* \equiv \xi, \quad (11)$$

$$180 \quad \gamma_s^* = \begin{cases} \frac{\lambda^\xi}{\gamma^{-1} - \frac{1}{\xi}(1-\lambda^\xi)}, & \xi \neq 0 \\ \frac{1}{\gamma^{-1} - \log(\lambda)}, & \xi = 0. \end{cases} \quad (12)$$

181 That is the conditions in (10) are fulfilled.
 182

183 Summarizing we have developed an IF model with only one spatially varying pa-
 184 rameter, the threshold u_s and the other parameters ξ, γ, λ constant over the region.
 185 Note, that we choose λ to be constant in the first place and therefore, obtain a site-
 186 specific threshold. This is different from the model proposed by *Madsen and Rosbjerg*
 187 [1997], where u_s is a priori fixed and only the shape parameter ξ is constant over the
 188 region, whereas σ and λ vary over the region, which violates relationship (2). More-
 189 over, the model is only an IF model for the excesses, whereas our model is an IF model
 190 for both the excesses and the exceedances.

191 We get the following GP model for the excesses:

$$192 \quad P(Y_s \leq y | Y_s \geq 0) = G_{\xi, \gamma, u_s}(y). \quad (13)$$

193 Now we can rewrite equation (1) for the $1/\alpha$ return level at site s , as

$$194 \quad q_\alpha(s) = \begin{cases} u_s \left(1 + \gamma \ln(\lambda/\alpha) \right), & \xi = 0, \\ u_s \left(1 - \frac{\gamma}{\xi} \left[1 - \left(\frac{\alpha}{\lambda} \right)^{-\xi} \right] \right), & \xi \neq 0. \end{cases} \quad (14)$$

195 As in equation (4), we see the factorization in a site specific index flood and a site
196 independent general quantile function.

2.2. Nonstationary climate

197 There is no general theory for the estimation of extreme quantiles of nonstationary
198 data. Approaches to account for long term trends in extremes are mostly ad hoc *Coles*
199 [2001]. The classical way to incorporate this nonstationarity in the POT approach, is
200 to keep the threshold constant and model the changing exceedance frequency by an
201 inhomogeneous Poisson process and the excesses by a GP distribution with time de-
202 pendent parameters [*Smith, 1989b; Coles, 2001; Yiou et al., 2006; Bengtsson and Nilsson,*
203 2007].

204 We follow a different route, which circumvents the inhomogeneous Poisson process
205 by considering a time dependent threshold, see e.g. *Coelho et al. [2008]* and *Kyselý et*
206 *al. [2010]*. A natural way to determine this varying threshold is quantile regression,
207 which can be described as a way to identify the temporal evolution of a given quantile
208 in a smooth parametric way, see e.g. *Koenker [2005]; Friederichs [2010]* and *Kyselý et al.*
209 [2010]. Quantile regression is further discussed in section 3.1. When we take a time de-
210 pendent high quantile, given by quantile regression, instead of a constant quantile, we
211 can assume that λ is constant over space and time. The time dependent GP distribution
212 is used to describe the excesses of the time varying threshold.

213 *Hanel et al. [2009]* generalize the IF assumption to the nonstationary block maxima
214 setting. Following them we generalize (5) in a similar way, which means that, after scal-
215 ing by a time dependent index flood, for every time point the site specific distribution

216 functions are constant over the region, i.e. $\forall s \in \mathcal{S}, \forall t \in \mathcal{T}$

$$217 \quad P \left(\frac{X_s(t)}{\eta_s(t)} \leq x | X_s(t) \geq u_s(t) \right) = \psi_t(x), \quad (15)$$

218 where ψ_t is independent of the site s . As in the stationary case we take the threshold as
219 index flood:

$$220 \quad \eta_s(t) = u_s(t).$$

221 Now we can generalize (9) in view of (15) to

$$222 \quad \tilde{\zeta}_s(t) \equiv \tilde{\zeta}(t), \quad \frac{\sigma_s(t)}{u_s(t)} \equiv \gamma(t), \quad (16)$$

223 and equation (14) can be generalized to the non-stationary setting:

$$224 \quad q_\alpha(s, t) = \begin{cases} u_s(t) \left(1 - \frac{\gamma(t)}{\tilde{\zeta}(t)} \left[1 - \left(\frac{\alpha}{\lambda} \right)^{-\tilde{\zeta}(t)} \right] \right), & \tilde{\zeta}(t) \neq 0, \\ u_s(t) \left(1 + \gamma(t) \ln(\lambda/\alpha) \right), & \tilde{\zeta}(t) = 0. \end{cases} \quad (17)$$

225
226 As in the stationary case, we can see the factorization into a time and site dependent
227 index flood and a quantile function, which depends on time only.

3. Estimation of the model parameters

228 We have chosen the threshold as a time dependent high quantile. For the estimation
229 of this quantile we use quantile regression, which is outlined in section 3.1. Section
230 3.2 illustrates the composite likelihood framework for estimating the time-dependent
231 parameters of the excess distribution.

3.1. Threshold estimation

232 Quantile regression relies on the fact that a sample quantile can be viewed as a solu-
233 tion of an optimization problem, which can be solved efficiently using linear program-
234 ming, as shown in *Koenker and Bassett [1978]*. When we fix $s \in \mathcal{S}$, we can obtain the

235 τ -th sample quantile of the observations $x_s = (x_{s,1}, \dots, x_{s,T})$ at site s as

$$236 \quad \arg \min_{\beta \in \mathbb{R}} \sum_{t=1}^T \rho_{\tau}(x_{s,t} - \beta), \quad (18)$$

237 where

$$238 \quad \rho_{\tau}(v) = \begin{cases} v(\tau - 1), & v < 0, \\ v\tau, & v \geq 0. \end{cases}$$

239 In linear quantile regression it is assumed, that the τ -th conditional quantile function
240 for given covariates z has a linear structure, i.e.

$$241 \quad Q_{x_s}(\tau|z) = z^T \beta(\tau), \quad (19)$$

242 e.g. a linear trend in time would be given by

$$243 \quad Q_{x_s}(\tau|t) = \beta_0(\tau) + t \cdot \beta_1(\tau).$$

244 In view of (18) *Koenker and Bassett [1978]* propose

$$245 \quad \arg \min_{\beta_0, \beta_1 \in \mathbb{R}} \sum_{t=1}^T \rho_{\tau}(x_{s,t} - \beta_0 - t\beta_1)$$

246 as estimator for $\beta(\tau)$. For details of the transformation of this optimization problem
247 into a linear program, see *Koenker [2005]*.

248 Note, that λ was defined as the mean number of exceedances in a block. If the linear
249 quantile function (19) holds, we have in fact the following relationship between τ and
250 λ ,

$$251 \quad (1 - \tau) \cdot T / \#N_B = \lambda,$$

252 where $\#N_B$ is the number of blocks.

3.2. Excess distribution estimation

253 Maximum likelihood (ML) estimation is a common approach to estimate the param-
254 eters in a statistical model. The ML framework has attractive asymptotic properties.

255 Moreover, it is very flexible, e.g. it is convenient to incorporate covariates. For these
 256 reasons several authors recommend it for the estimation of extreme quantiles, espe-
 257 cially when trends occur, see e.g. *Coles* [2001].

258 In order to apply the ML method, one needs the full likelihood function of the pre-
 259 cipitation extremes, over all times and sites. Because of the spatial dependence, this
 260 requires the joint distribution of the excesses at all sites, which is difficult to describe
 261 because of the large dimensionality and estimation would be virtually impossible. One
 262 interesting way to proceed without the knowledge of the full dependence structure is
 263 to use a simplified likelihood. A class of such simplified likelihoods is summarized in
 264 the framework of composite likelihood, see e.g. *Varin et al.* [2011]. In this study we
 265 focus in particular on the independence likelihood, see also *Chandler and Bate* [2007].
 266 The independence likelihood is the likelihood, as the name suggests, that would be
 267 obtained if the excesses at different sites were independent. We want to emphasize,
 268 that we focus on local quantiles and their spatial variation over a region, in which case
 269 the independence likelihood gives reasonable results, compare *Cooley et al.* [2007] and
 270 *Blanchet and Lehning* [2010]. This is, however, not the case if dependence parameters
 271 are of interest, as in *Padoan et al.* [2010], where a pairwise composite likelihood is used.

272 In the nonstationary IF model, the parameters γ and ξ of the excess distribution
 273 depend on time. We postulate a certain structure for these parameters, e.g.

$$274 \quad \gamma(t) = \gamma_1 + \gamma_2 \cdot (t - \bar{t}), \quad \xi(t) = \xi_1,$$

275 where \bar{t} is the mean of the time points, so that γ_1 is the average of $\gamma(t)$ over t . Let
 276 $\theta = (\gamma_1, \gamma_2, \xi_1)$ be the vector of parameters, that has to be estimated. The independence

277 likelihood is then given by:

$$278 \quad \mathcal{L}_I(\theta, \mathbf{Y}) = \prod_{t \in \mathcal{T}} \prod_{\substack{s \in \mathcal{S} \\ y_s(t) \geq 0}} \frac{1}{\gamma(t)u_s(t)} \cdot \left[1 + \frac{\tilde{\zeta}(t)y_s(t)}{\gamma(t)u_s(t)} \right]^{(-1/\tilde{\zeta}(t)-1)},$$

279 where the condition on $y_s(t) \geq 0$ reflects that we only consider peaks over the thresh-
280 old. Note, that by the choice of the quantile the threshold has been fixed beforehand.

281 The maximum independence likelihood estimator (MILE) is the parameter $\hat{\theta}_I$ which
282 maximizes $\mathcal{L}_I(\theta, \mathbf{Y})$ or equivalently the independence log likelihood

$$283 \quad \ell_I(\theta, \mathbf{Y}) = - \sum_{t \in \mathcal{T}} \sum_{\substack{s \in \mathcal{S} \\ y_s(t) \geq 0}} \left[\ln(\gamma(t)u_s(t)) + \right. \\ 284 \quad \left. + \frac{1 + \tilde{\zeta}(t)}{\tilde{\zeta}(t)} \ln\left(1 + \frac{\tilde{\zeta}(t)y_s(t)}{\gamma(t)u_s(t)}\right) \right]. \quad (20) \\ 285$$

286 We have to optimize this function, with respect to the elements of θ . This can be done
287 using the Broyden-Fletcher-Goldfarb-Shanno (BFGS) method as implemented in the
288 `optim`-function of GNU R [R Development Core Team, 2011].

289 For testing the adequacy of the IF model, it is necessary to consider more general
290 models with a spatially dependent dispersion coefficient, e.g. $\gamma_s(t) = \gamma_s$ and $\tilde{\zeta}_s(t) = \tilde{\zeta}$.
291 The independence log likelihood for this model is obtained by replacing $\gamma(t)$ by γ_s and
292 $\tilde{\zeta}(t)$ by $\tilde{\zeta}$ in equation (20). The direct optimization of this likelihood with respect to the
293 $(S + 1)$ parameters is in the case of a large number of sites computationally very de-
294 manding. Therefore we exploit the structure of the independence likelihood by using
295 a profile likelihood approach. In the example above we can split, for a given shape pa-
296 rameter, the optimization over an S -dimensional space into S optimization problems in
297 one dimension, i.e. the maximization of the log likelihood for the excesses at site s with
298 respect to $\tilde{\zeta}_s$. This is usually much faster. If one does this on a grid of potential values

299 for the shape parameter one can see the structure of the profile likelihood. Moreover
 300 we can construct a convergent procedure, leading to the estimator for the shape param-
 301 eter. We recommend as initial value for this procedure the mean of the estimated shape
 302 parameters $\hat{\xi}_s$ of a site specific model. Another problem with the direct optimization
 303 might be the existence of local maxima in the likelihood; with the proposed approach
 304 we did not experience any problems with this issue.

305 The MILE $\hat{\theta}_I$ is asymptotically normal, see e.g. *Varin et al.* [2011]:

$$306 \quad \sqrt{\#\tilde{\mathcal{T}}}(\hat{\theta}_I - \theta) \xrightarrow{d} N\left(0, G^{-1}(\theta)\right),$$

307 where $\#\tilde{\mathcal{T}}$ is the number of days with one or more threshold exceedances and G is the
 308 Godambe information:

$$309 \quad G(\theta) = H(\theta)J^{-1}(\theta)H(\theta), \quad (21)$$

310 where $H(\theta)$ is minus the expected Hessian of ℓ_I at θ , also referred to as sensitivity
 311 matrix, and J is the variability matrix, i.e. the covariance matrix of the score $u(\theta, \mathbf{Y}) =$
 312 $\nabla_{\theta}\ell_I(\theta, \mathbf{Y})$. In the case of spatial independence, we have $H(\theta) = J(\theta)$ and the Godambe
 313 information reduces to the Fisher information, i.e. $G(\theta) = H(\theta)$. Here H is estimated
 314 as its observed value at $\hat{\theta}_I$, and J as

$$315 \quad J = \frac{1}{\#\tilde{\mathcal{T}}} \sum_{t \in \tilde{\mathcal{T}}} u(\hat{\theta}_I, y(t)) u(\hat{\theta}_I, y(t))',$$

316 where $y(t) = (y_1(t), \dots, y_S(t))'$ and $u(\hat{\theta}_I, y(t))$ is the contribution of day t to $u(\hat{\theta}, \mathbf{Y})$.
 317 The latter estimate makes use of the fact that the excesses on different days are in-
 318 dependent, see e.g. *Chandler and Bate* [2007] and *Varin et al.* [2011]. An estimate of
 319 the Godambe information $\hat{G}(\theta)$ is obtained by plugging in the estimates \hat{H} and \hat{J} in

320 equation (21). This estimate \hat{G} is used to assess the uncertainty of the parameters (and
 321 quantiles) of the excess distribution, see section 4

4. Model selection for the excess distribution

322 In this section we describe the methods used, to investigate the temporal behavior
 323 of the dispersion coefficient and the shape parameter as well as the adequacy of the IF
 324 model.

325 Information criteria are used as indication of the suitability of a specific model. *Varin*
 326 *et al.* [2011] present composite likelihood adaptations of the Akaike information crite-
 327 rion (AIC) and the Bayesian information criterion (BIC), which are defined in the usual
 328 way

$$329 \quad AIC = -2\ell_I(\hat{\theta}_I, Y) + 2 \dim(\theta),$$

$$330 \quad BIC = -2\ell_I(\hat{\theta}_I, Y) + \log(\#\tilde{\mathcal{T}}) \dim(\theta),$$

332 where $\dim(\theta)$ is an effective number of parameters, which can be estimated as

$$333 \quad \dim(\theta) = \text{tr} \left(H(\theta) G(\theta)^{-1} \right).$$

334 Moreover, we will test our assumptions using nested models. This means, that we
 335 consider subsets M_0 of the full model M_1 by constraining q components of the param-
 336 eter vector θ . For instance we may partition $\theta = (\psi, \phi)$ such that the q -dimensional
 337 component ψ is zero under M_0 . To test this hypothesis, we use the independent likeli-
 338 hood ratio statistic, which is a special case of a composite likelihood ratio (CLR) statistic
 339 [*Chandler and Bate, 2007; Varin et al., 2011*]:

$$340 \quad W = 2 \left[\ell_I(\hat{\theta}_{M_1}; y) - \ell_I(\hat{\theta}_{M_0}; y) \right], \quad (22)$$

341 where $\hat{\theta}_{M_1}$ ($\hat{\theta}_{M_0}$) denotes the MILE of model M_1 (M_0). *Varin et al.* [2011] present the
 342 following asymptotic result for W under the null hypothesis

$$343 \quad W \xrightarrow{d} \sum_{j=1}^q \lambda_j Z_j^2, \quad (23)$$

344 where the Z_j are independent, standard normal variates and $\lambda_1, \dots, \lambda_q$ are the eigen-
 345 values of

$$346 \quad (G_{M_1}^{-1})_{\psi} \left((H_{M_1}^{-1})_{\psi} \right)^{-1}.$$

347 Here $(G_{M_1}^{-1})_{\psi}$ denotes the submatrix of the inverse Godambe information for the full
 348 model M_1 pertaining to the parameter vector ψ and $(H_{M_1}^{-1})_{\psi}$ is defined analogously.

349 In order to obtain the information criteria and the asymptotic distribution of W under
 350 the null hypothesis, we need to estimate the Godambe information, which is difficult
 351 when the number of parameters is large. Hence it is not feasible to examine the ap-
 352 propriateness of the IF assumption for regions with many sites, based on the Godambe
 353 information.

354 One possibility to obtain p -values for the test statistic W , without estimating the Go-
 355 dambe information, is to apply a bootstrap procedure, see e.g. *Varin et al.* [2011]. We
 356 follow *Hanel et al.* [2009] and use a semiparametric bootstrap approach, to take the de-
 357 pendence structure into account, without explicitly modeling this. The challenge is to
 358 produce bootstrap samples according to the null hypothesis, which exhibit approxi-
 359 mately the same spatial dependence structure as the original data set. We assume that
 360 the underlying spatial dependence is not changing over time, i.e. only the marginal
 361 distributions are changing. One could think of a constant copula generating the de-

pendence structure, that is for fixed t

$$P(Y_s(t) \leq y_{s,t} \forall s) = C(G_{1,t}(y_{1,t}), \dots, G_{S,t}(y_{S,t})),$$

where $G_{s,t} = G_{\sigma_s(t), \hat{\zeta}_s^1(t)}$, and C a copula, for details on copula see e.g. *Nelson* [2006]. We generate the bootstrap samples in three steps. In the first step we transform the sample of the excesses $Y_s(t)$ into a sample that follows approximately the standard exponential distribution

$$Z_s(t) = \begin{cases} \frac{1}{\hat{\zeta}_s^1(t)} \ln\left(1 + \frac{\hat{\zeta}_s^1(t) Y_s(t)}{\hat{\sigma}_s^1(t)}\right), & \hat{\zeta}_s^1(t) \neq 0, \\ \frac{Y_s(t)}{\hat{\sigma}_s^1(t)}, & \hat{\zeta}_s^1(t) = 0, \end{cases} \quad (24)$$

where $\hat{\sigma}_s^1(t)$ and $\hat{\zeta}_s^1(t)$ are the estimated scale and shape parameters under the full model M_1 . In the second step, we sample with replacement monthly blocks of the whole spatial domain from $Z_s(t)$ to obtain a new sample $\tilde{Z}_s(t)$ with approximately standard exponential margins and the same spatial dependence structure as that of $Z_s(t)$. In the third step we use the estimated scale and shape parameter under the null hypothesis, denoted as $\hat{\sigma}_s^0(t)$ and $\hat{\zeta}_s^0(t)$, respectively, to transform the sample $\tilde{Z}_s(t)$ to a bootstrap sample of the excesses

$$\tilde{Y}_s(t) = \begin{cases} \frac{\hat{\sigma}_s^0(t)}{\hat{\zeta}_s^0(t)} [\exp(\hat{\zeta}_s^0(t) \tilde{Z}_s(t)) - 1], & \hat{\zeta}_s^0(t) \neq 0, \\ \tilde{Z}_s(t) \hat{\sigma}_s^0(t), & \hat{\zeta}_s^0(t) = 0. \end{cases} \quad (25)$$

The $\tilde{Y}_s(t)$ follow approximately the GP model M_0 and mimic the spatial dependence structure of the original excesses.

From a number of Monte Carlo experiments, *Kyselý* [2007, 2009] concluded that the (non-parametric) bootstrap generally resulted in too narrow confidence intervals for large quantiles of the distributions, that are commonly used to describe the distribution of precipitation extremes. This has been attributed to the skewness of the estimators of the model parameters in the case of small and moderate sample sizes. This objection

384 might be weakened, when using RFA methods, because then the estimation is based
385 on much more data.

5. Application to precipitation data

386 We applied the regional peaks-over-threshold method to observed precipitation data
387 from the Netherlands. We used the daily, gridded E-OBS data (version 5.0), which
388 were made available by the European funded project ENSEMBLES [Haylock *et al.*, 2008].
389 We consider winter (DJF) precipitation for $25\text{ km} \times 25\text{ km}$ grid squares centered in the
390 Netherlands, for the period December 1, 1950 to February 28, 2010. In total we have 69
391 grid boxes and 60 winter seasons of daily measurements for each grid box.

392 The Netherlands has a maritime climate with relatively mild and humid winters.
393 Figure 1 shows the mean over the considered period of the largest daily precipitation
394 value in winter (winter maximum) for each grid box. The spatial variation in Figure 1
395 is small, 80% of the values lie between 18.2 and 20.4 mm. Previous studies propose to
396 view the Netherlands as a homogeneous region for which the IF assumption applies,
397 see e.g. *Overeem et al.* [2008] and *Hanel et al.* [2009].

398 Daily precipitation in the winter season exhibits some temporal dependence, also at
399 high levels. The relation between the GEV and GP distribution parameters (Equation
400 (2)) relies on the independence assumption as does the estimation of the variability
401 matrix J , therefore, it is necessary to select a subset of independent events. This is
402 usually achieved by specifying a minimum separation time between exceedances over
403 the threshold [e.g. *Kyselý et al.*, 2010].

404 We decluster the original data rather than the exceedances, i.e. we look at blocks
405 of length one plus the minimum separation time and replace all but the maximum

406 values of these blocks by zero and determine the threshold for these declustered data,
407 as described in section 3.1. It follows that the exceedances are declustered with the
408 same minimum separation time. The advantage of this procedure over declustering
409 the exceedances directly, is that the expected number of exceedances per block will be
410 approximately constant over the region, which is a basic assumption of our model. As
411 the persistence of rain events is rather short, we specify the minimum separation time
412 to be one day.

413 We choose the threshold to be the 96% linear regression quantile. Hence, we expect
414 on average 3.61 exceedances per grid box and winter season. Figure 2 shows for each
415 grid box the mean of this threshold for the 1950–2010 period. The trend in the threshold
416 for the 1950–2010 period is positive over the whole domain, see Figure 3, but is rela-
417 tively small in the southeastern part of the country and large (up to 40%) in the west
418 and northern parts. *Buishand et al.* [2012] found a significant positive trend in the mean
419 precipitation for the winter half year (October – March) in the Netherlands during the
420 period 1951 – 2009. A clear spatial gradient was, however, not observed in the trend of
421 the mean winter precipitation.

422 We test the hypothesis that the event times come from a Poisson process individually
423 for each grid box by the dispersion index (DI) test. The DI test exploits the fact, that
424 the variance and the mean of the Poisson distribution are the same, see *Cunnane* [1979]
425 for details. The Poisson assumption is rejected at the 5% significance level in two of
426 the 69 grid boxes, which is in good agreement with the expected number of rejected
427 grid boxes under the Poisson assumption. If the exceedance times come from a homo-
428 geneous Poisson process, these should be distributed uniformly on any time interval,

429 see e.g. *Cox and Lewis* [1966]. The Kolmogorov-Smirnov test does not reject uniformity in
430 any grid box.

431 We exploit the fact that event times, coming from a Poisson process, are uniformly
432 distributed over time. The resulting p-values of a Kolmogorov-Smirnov test on the
433 uniformity are shown in Figure 4.

434 We consider four different models for the excess distribution, three based on the IF
435 approach, **A** – **A''** in Table 1, and one with a spatially varying dispersion coefficient and
436 constant shape parameter, model **B**.

437 In a first step we want to infer which of the IF models is the best to describe the data.
438 For a first indication the information criteria are computed, as outlined in section 4, for
439 each of the three IF models, see Table 2. We see from both the composite AIC and the
440 composite BIC, that the incorporation of a trend in the dispersion coefficient γ (model
441 **A'**) does not result in a better model. One can see on the other hand, that according to
442 the AIC model **A''**, which has a (linear) trend in the shape parameter, is selected. That
443 contrasts with the selection of the simplest model **A**, by means of the BIC.

444 The shape parameter is crucial for the estimation of very high quantiles. Model **A**
445 estimates the shape parameter to be 0.03, i.e. just in the Fréchet domain. Model **A''**
446 estimates a large drop in the shape parameter from 0.10 to -0.09, which would mean
447 a change from the Fréchet family to the Weibull family. In order to gain more insight
448 in the temporal behavior of the shape parameter, we compute the shape parameter for
449 overlapping 20 year subsamples of the data, using model **A**, which has no trend in
450 the model parameters. It appears that a large part of the negative trend in the shape
451 parameter in model **A''** is due to one specific event, namely the extreme rainfall of

452 December 3, 1960, compare also *Buishand* [1984] and *Van den Brink and Können* [2011],
453 resulting in a large drop of the 20 year window estimates in the year 1971, as observed
454 in Figure 5.

455 The quantile estimates, obtained from model **A**, are increasing due to the positive
456 trend in the threshold. Because of the connection of the scale parameter with the thresh-
457 old, see equation (16), the positive trend in the threshold leads to a positive linear trend
458 in the scale parameter. In contrast to the previous model, we obtain from model **A''**,
459 quantile estimates, that exhibit a phase transition. While the 2 year return level is still
460 increasing due to the positive trend in the threshold, we have that the 25 year return
461 level is decreasing due to the negative trend in the common shape parameter. The 5
462 year return level is approximately constant, see Figure 6. An interpretation of this is
463 much more complex, than for the quantile estimates, stemming from model **A**.

464 When we carry out the composite likelihood ratio test, it turns out, that neither the
465 trend in the dispersion coefficient nor the trend in the shape parameter are significant,
466 although the p -values are quite different for these trends, see Table 3. We can also
467 see from Table 3, that the bootstrap procedure gives similar results as the use of the
468 asymptotic result in equation (23).

469 In the second step we want to test the IF assumption. Therefore we compute the
470 composite likelihood ratio test for the full model **B** and the nested model **A**. As earlier
471 explained, we can not estimate the Godambe information well for model **B**. Hence,
472 we proceed only with the bootstrap procedure. We obtain an p -value of 0.103 for 2500
473 bootstrap samples. This means, that the IF assumption does not have to be rejected.
474 Note, because of the large difference in the number of parameters between model **B**

475 and model **A**, the composite likelihood ratio test will not have much power due to the
476 great number of alternatives. This can be considered as an intrinsic problem, when
477 comparing regional models with site dependent parameters.

478 Figure 7 compares for a particular site the estimated return levels of the excess distri-
479 bution based on the site specific approach with those obtained from the IF assumption.
480 Pointwise confidence bands for the return levels based on the asymptotic normality of
481 the MILE are also given. The quantile estimates for the two methods are quite similar,
482 but the IF approach reduces the uncertainty in the estimation to half the uncertainty of
483 the site specific approach.

6. Conclusions

484 An index flood approach for nonstationary peaks-over-threshold data has been de-
485 veloped. The threshold is chosen to be a large quantile that varies over time, which
486 is also taken as the index flood. The peaks exceeding the threshold are described by
487 Generalized Pareto distributions. The index flood assumption implies that the ratio
488 of the scale parameter to the threshold and the shape parameter are constant over the
489 region but may vary over time.

490 The approach was applied to gridded, observed daily precipitation data from the
491 Netherlands for the winter season. A linear increase in the threshold was found, which
492 was most pronounced in the western and northern parts of the country. This increase
493 in the threshold leads to an increase in the scale parameter, because of the index flood
494 assumption. No evidence was found for a change in the ratio of the scale parameter
495 to the threshold. Though a large negative trend in the shape parameter was observed,

496 this trend turned out to be mainly due to one exceptional event. Therefore, the extreme
497 quantiles increase in the same way as the threshold.

498 Although the uncertainty in the estimation of the excess distribution was cut by
499 half compared to a site specific estimation procedure, the remaining uncertainty is still
500 substantial. The uncertainty could be possibly further reduced by considering longer
501 records or by extending the region. For instance, one could think of including the
502 neighboring part of North Germany in the analysis. The different trends in the index
503 flood indicate, however, that one should be very careful with extending the region.
504 Apart from analyzing more data, the estimation uncertainty might also be reduced by
505 maximizing a pairwise likelihood that partly accounts for spatial dependence rather
506 than the independent likelihood.

507 The validity of the bootstrap might be questionable and should be assessed by a
508 Monte Carlo experiment, which includes the spatial dependence. However, this is
509 for peaks-over-threshold data much more computational demanding than for block
510 maxima.

511 **Acknowledgments.** The research was supported by the Dutch research program
512 Knowledge for Climate. We acknowledge the E-OBS dataset from the EU-FP6 project
513 ENSEMBLES (<http://ensembles-eu.metoffice.com>) and the data providers in the
514 ECA&D project (<http://eca.knmi.nl>). All calculations were performed using the R
515 environment (<http://www.r-project.org>).

References

- 516 Beguería, S., M. Angulo-Martínez, S. M. Vicente-Serrano, J. I. López-Moreno, and A. El-
517 Kenawy (2011), Assessing trends in extreme precipitation events intensity and mag-
518 nitude using non-stationary peaks-over-threshold analysis: a case study in North-
519 east Spain from 1930 to 2006. *International Journal of Climatology*, 31(14): 2102–2114,
520 doi:10.1002/joc.2218.
- 521 Bengtsson, A. and C. Nilsson (2007), Extreme value modelling of storm damage in
522 Swedish forests. *Nat. Hazards Earth Syst. Sci.*, 7:515–521.
- 523 Blanchet, J. and M. Lehning (2010), Mapping snow depth return levels: smooth
524 spatial modeling versus station interpolation. *Hydrology and Earth System Sciences*,
525 14(12):2527–2544, doi:10.5194/hess-14-2527-2010.
- 526 Brown, S. J., J. Caesar, and C. A. T. Ferro (2008), Global changes in extreme daily
527 temperature since 1950. *J. Geophys. Res.*, 113(D5):D05115, doi:10.1029/2006JD008091.
- 528 Buishand, T. A. (1984), Zware neerslag in het winterhalfjaar. *Cultuurtechnisch Tijdschrift*,
529 23(5). In Dutch.
- 530 Buishand, T. A. (1989), Statistics of extremes in climatology. *Statistica Neerlandica*,
531 43(1):1–30, doi:10.1111/j.1467-9574.1989.tb01244.x.
- 532 Buishand, T. A., G. De Martino, H. Spreeuw, and T. Brandsma (2012), Homogeneity of
533 precipitation series in the Netherlands and their trends in the past century. *Internation-*
534 *al Journal of Climatology*, Accepted.
- 535 Chandler, R. E. and S. Bate (2007), Inference for clustered data using the independence
536 loglikelihood. *Biometrika*, 94(1):167–183, doi:10.1093/biomet/asm015.

- 537 Coelho, C. A. S., C. A. T. Ferro, D. B. Stephenson, and D. J. Steinskog (2008), Meth-
538 ods for exploring spatial and temporal variability of extreme events in climate data.
539 *Journal of Climate*, 21(10):2072–2092, doi:10.1175/2007JCLI1781.1.
- 540 Coles, S. (2001), *An Introduction to Statistical Modeling of Extreme Values*. Springer, Lon-
541 don.
- 542 Cooley, D., D. Nychka, and P. Naveau (2007), Bayesian spatial modeling of extreme
543 precipitation return levels. *Journal of the American Statistical Association*, 102(479):824–
544 840, doi:10.1198/016214506000000780.
- 545 Cox, D. R. and P. A. W. Lewis (1966), *The Statistical Analysis of Series of Events*. Methuen,
546 London.
- 547 Cunnane, C. (1979), A note on the Poisson assumption in partial duration series mod-
548 els. *Water Resour. Res.*, 15(2):489–494, doi:10.1029/WR015i002p00489.
- 549 Cunnane, C. (1988), Methods and merits of regional flood frequency analysis. *Journal*
550 *of Hydrology*, 100(1-3):269 – 290, doi:10.1016/0022-1694(88)90188-6.
- 551 Dalrymple, T. (1960), Flood-frequency analyses, manual of hydrology: Part 3. *USGS*
552 *Water Supply Paper*, 1543-A.
- 553 Embrechts, P., C. Klüppelberg, and T. Mikosch (1997), *Modelling Extremal Events*.
554 Springer, Berlin.
- 555 Fowler, H. J., M. Ekström, C.G. Kilsby, and P.D. Jones (2005), New estimates of fu-
556 ture changes in extreme rainfall across the UK using regional climate model inte-
557 grations. 1. assessment of control climate. *Journal of Hydrology*, 300(1-4):212 – 233,
558 doi:10.1016/j.jhydrol.2004.06.017.

- 559 Friederichs, P. (2010), Statistical downscaling of extreme precipitation events using
560 extreme value theory. *Extremes*, 13:109–132, doi:10.1007/s10687-010-0107-5.
- 561 Hanel, M., T. A. Buishand, and C. A. T. Ferro (2009), A nonstationary index flood
562 model for precipitation extremes in transient regional climate model simulations. *J.*
563 *Geophys. Res.*, 114(D15):D15107, doi:10.1029/2009JD011712.
- 564 Haylock, M. R., N. Hofstra, A. M. G. Klein Tank, E. J. Klok, P. D. Jones, and
565 M. New (2008), A European daily high-resolution gridded data set of surface
566 temperature and precipitation for 1950-2006. *J. Geophys. Res.*, 113(D20):D20119,
567 doi:10.1029/2008JD010201.
- 568 Hosking, J. R. M., and J. R. Wallis (1997), *Regional Frequency Analysis*. Cambridge
569 University Press, Cambridge, UK.
- 570 Kharin, V. V. and F.W. Zwiers (2005), Estimating extremes in transient climate change
571 simulations. *Journal of Climate*, 18(8):1156–1173, doi:10.1175/JCLI3320.1.
- 572 Klein Tank, A. M. G., and G. P. Können (2003), Trends in indices of daily temperature
573 and precipitation extremes in Europe, 1946-99. *Journal of Climate*, 16(22):3665–3680,
574 doi:10.1175/1520-0442(2003)016<3665:TIHODT>2.0.CO;2.
- 575 Koenker, R. (2005), *Quantile Regression*. Cambridge University Press, Cambridge, UK.
- 576 Koenker, R. and G. Bassett Jr. (1978), Regression quantiles. *Econometrica*, 46(1):33–50.
- 577 Kysely, J. (2007), A cautionary note on the use of nonparametric bootstrap for
578 estimating uncertainties in extreme-value models. *Journal of Applied Meteorology*,
579 47:3236–3251, doi:10.1175/2008JAMC1763.1.
- 580 Kysely, J. (2009), Coverage probability of bootstrap confidence intervals in heavy-
581 tailed frequency models, with application to precipitation data. *Theor Appl Climatol*,

- 582 101:345–361, doi:10.1007/s00704-009-0190-1.
- 583 Kyselý, J., J. Picek, and R. Beranová (2010) Estimating extremes in climate change
584 simulations using the peaks-over-threshold method with a non-stationary threshold.
585 *Global and Planetary Change*, 72(1-2):55 – 68, doi:10.1002/joc.1874.
- 586 Madsen, H., P. F. Rasmussen, and D. Rosbjerg (1997a), Comparison of an-
587 nual maximum series and partial duration series methods for modeling ex-
588 treme hydrologic events: 1. at-site modeling. *Water Resour. Res.*, 33(4):747–757,
589 doi:10.1029/96WR03848.
- 590 Madsen, H., C. P. Pearson, and D. Rosbjerg (1997b), Comparison of annual maximum
591 series and partial duration series methods for modeling extreme hydrologic events:
592 2. regional modeling. *Water Resour. Res.*, 33(4):759–769, doi:10.1029/96WR03849.
- 593 Madsen, H. and D. Rosbjerg (1997), The partial duration series method in regional
594 index-flood modeling. *Water Resour. Res.*, 33(4):737–746, doi:10.1029/96WR03847.
- 595 Milly, P. C. D., J. Betancourt, M. Falkenmark, R.M. Hirsch, Z.W. Kundzewicz, D.P. Let-
596 tenmaier, and R.J. Stouffer (2008), Stationarity is dead: whither water management?
597 *Science*, 319(5863):573–574, doi:10.1126/science.1151915.
- 598 Nelsen, R. B. (2006), *An Introduction to Copulas*. Springer, New York.
- 599 Overeem, A., T. A. Buishand, and I. Holleman (2008), Rainfall depth-duration-
600 frequency curves and their uncertainties *Journal of Hydrology*, 348:124–134,
601 doi:10.1016/j.jhydrol.2007.09.044
- 602 Padoan, S. A., M. Ribatet, and S. A. Sisson (2010), Likelihood-based inference for
603 max-stable processes. *Journal of the American Statistical Association*, 105(489):263–277,
604 doi:10.1198/jasa.2009.tm08577.

- 605 R Development Core Team (2011), *R: A Language and Environment for Statistical*
606 *Computing. R Foundation for Statistical Computing, Vienna, Austria.*
- 607 Reiss, R. D. and M. Thomas (2007), *Statistical Analysis of Extreme Values: with Applica-*
608 *tions to Insurance, Finance, Hydrology and Other Fields.* Birkhäuser, Basel, 3rd edition.
- 609 Robinson, J. S. and M. Sivapalan (1997), An investigation into the physical causes of
610 scaling and heterogeneity of regional flood frequency. *Water Resour. Res.*, 33(5):1045–
611 1059, doi:10.1029/97WR00044.
- 612 Rosbjerg, D., H. Madsen, and P. F. Rasmussen (1992), Prediction in partial duration se-
613 ries with generalized Pareto-distributed exceedances. *Water Resour. Res.*, 28(11):3001–
614 3010, doi:10.1029/92WR01750.
- 615 Smith, J. A. (1989a), Regional flood frequency analysis using extreme or-
616 der statistics of the annual peak record *Water Resour. Res.*, 25(2):311–317,
617 doi:10.1029/WR025i002p00311.
- 618 Smith, R. L. (1986), Extreme value theory based on the r largest annual events. *Journal*
619 *of Hydrology*, 86(1-2):27 – 43, doi:10.1016/0022-1694(86)90004-1.
- 620 Smith, R. L. (1989b), Extreme value analysis of environmental time series: An applica-
621 tion to trend detection in ground-level ozone. *Statistical Science*, 4(4):367–377.
- 622 Turco, M. and M. C. Llasat (2011), Trends in indices of daily precipitation extremes
623 in Catalonia (NE Spain), 1951 - 2003. *Natural Hazards and Earth System Science*,
624 11(12):3213–3226, doi:10.5194/nhess-11-3213-2011.
- 625 Van den Brink, H. W. and G. P. Können (2011), Estimating 10000-year return
626 values from short time series. *International Journal of Climatology*, 31(1):115–126,
627 doi:10.1002/joc.2047.

- 628 Varin, C., N. Reid, and D. Firth (2011), An overview of composite likelihood methods.
629 *Statistica Sinica*, 21:5–42.
- 630 Wang, Q.J. (1991), The POT model described by the generalized Pareto distribution
631 with Poisson arrival rate. *Journal of Hydrology*, 129(1–4):263 – 280, doi:10.1016/0022-
632 1694(91)90054-L.
- 633 Wigley, T. (2009), The effect of changing climate on the frequency of absolute extreme
634 events. *Climatic Change*, 97:67–76, doi:10.1007/s10584-009-9654-7.
- 635 Yiou, P., P. Ribereau, P. Naveau, M. Nogaj, and R. Brázdil (2006), Statistical analy-
636 sis of floods in Bohemia (Czech Republic) since 1825. *Hydrological Sciences Journal*
637 51(5):930–945, doi:10.1623/hysj.51.5.930

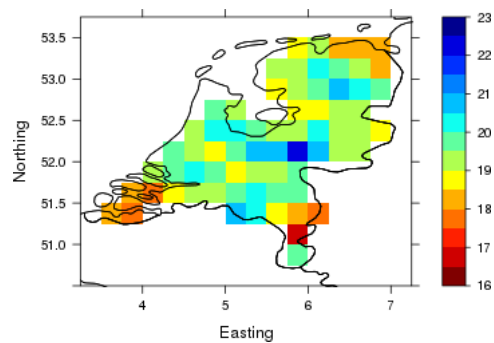


Figure 1. Mean of the winter maxima in mm

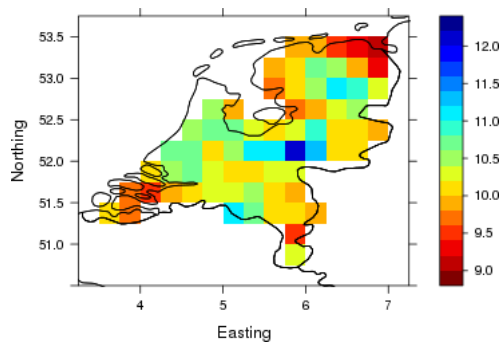


Figure 2. Mean of the threshold for the 1950–2010 period in mm

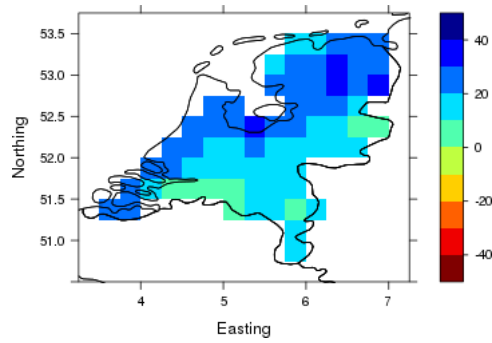


Figure 3. Trend in the threshold for the 1950–2010 period in %. The trend was defined as the difference between the last and the first value of the threshold divided by the mean value of the threshold.

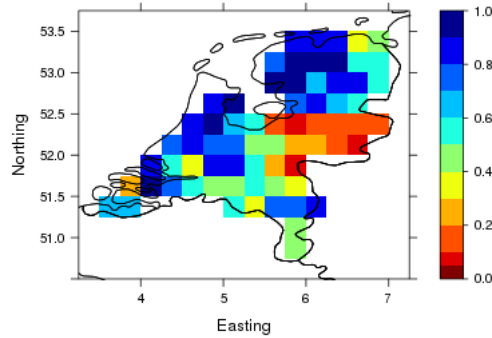


Figure 4. p-values of the uniformity for the event times

Table 1. Overview of models used

Model	dispersion	shape
A	γ	ξ
A'	$\gamma_1 + \gamma_2 * (t - \bar{t})$	ξ
A''	γ	$\xi_1 + \xi_2 * (t - \bar{t})$
B	$\gamma_1, \dots, \gamma_S$	ξ

Table 2. Information criteria for the IF models^a.

Model	AIC	BIC
A	78387.28	78715.59
A'	78435.60	78880.41
A''	78333.28	78748.95

^aThe lowest AIC and BIC values are printed in bold.

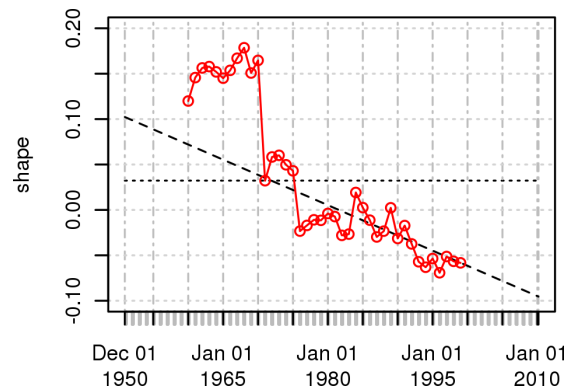


Figure 5. Evolution of the shape parameter over time (dotted - model A, dashed - model A'', solid red line with points - 20 year window estimates for model A)

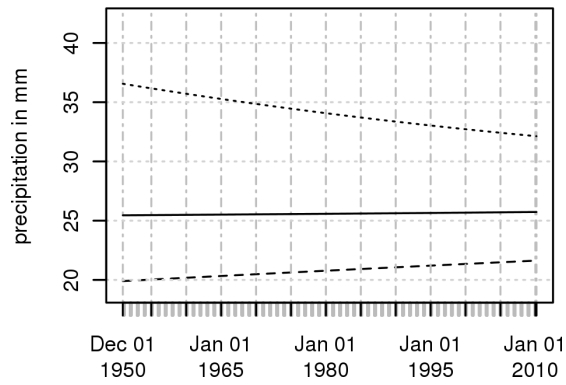


Figure 6. Trends of different return levels of daily precipitation for model A'' (dashed – 2 year, solid – 5 year, dotted – 25 year)

Table 3. *p*-values of the CLR-test against model A (2500 samples)

Model	asymptotic	bootstrap
A'	82.9%	81.3%
A''	26.7%	12.2%

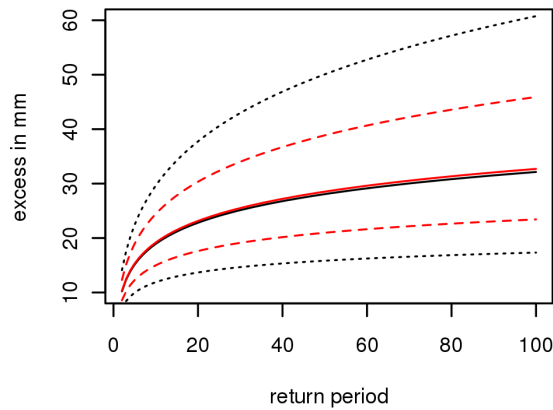


Figure 7. Estimated return levels of the excesses with 95% pointwise confidence bands for the year 1980 at the grid box around De Bilt (black – site specific, red – IF)